We are IntechOpen, the world's leading publisher of Open Access books Built by scientists, for scientists

6,900
Open access books available

185,000
International authors and editors

200M
Downloads

Our authors are among the

154
Countries delivered to

TOP 1%
most cited scientists

12.2%
Contributors from top 500 universities



WEB OF SCIENCE™

Selection of our books indexed in the Book Citation Index in Web of Science™ Core Collection (BKCI)

Interested in publishing with us?
Contact book.department@intechopen.com

Numbers displayed above are based on latest data collected.
For more information visit www.intechopen.com



3

Circulation Type Blood Vessel Simulator Made by Microfabrication

Takuma Nakano and Fumihito Arai
Nagoya University
Japan

1. Introduction

Recently, Japanese have causes of the death. Figure 1.1 was reported by Ministry of Health, Labour and Welfare in 2008 in Japan and which shows the cause of the death. As you can see, the causes of death are cancer, cardiac disease, cerebrovascular disease and etc.. We can categorize cardiac disease and cerebrovascular disease as blood vessel disease. Blood vessel disease is the second highest cause of the death. To treat the cancer and blood vessel disease, many engineering approaches have been studied about tissue engineering, medical treatment tools, rehearsal systems and synthetic vascular prostheses. For treatment of cancer, there are researches of endoscope and abdominoscope for less-invasive surgical operation. For treatment of blood vessel disease, there are researches of endoscope which can use in blood vessels and synthetic vascular prostheses for replacement operation. These researches have the common identity that is improvement of quality of life (QOL). But, these less-invasive operations are poor in extracting the organ size and controlling the posture of medical tools. To solve these problems, many researches from the other approaches are proposed. One of them is research about surgical simulators for rehearsal, practice and evaluation of real surgical operation. Generally, VR simulator and CFD analysis are famous as computer surgical simulator (Fig.1.2 (a) and (b)). These simulators enable to simulate surgical operation easily, and analyze fluid condition easily, however, these are poor in simulating pulsative system and not suitable to evaluate new treatment method using narrow vessels. Our surgical simulator (Endo Vascular Evaluator: EVE) has three-dimensional (3D) blood vessel models fabricated in tailor-made (Fig.1.2 (c)) (Ikeda et al., 2005). And, EVE enables to simulate pulsative system and catheter operation easily, but, not suitable to evaluate new treatment method using narrow vessels. There are two famous methods using narrow vessels. One is a method of necrotizing cancer cells in the part of liver as shown in Fig.1.3 (a) (trancecatheter arterial chemoembolization: TACE, TAE). The other is a method of administering medicine as shown in Fig.1.3 (b) (drug delivery systems:DDS). TAE method protocol is to release anticancer drug and gelatin sponge in blood vessels for stack, then stop the blood flow and the supply nourishment. Stacking gelatin sponge has a possibility of effect to normal cells. Thus, gelatin sponge are needed to release from catheter, and it is very difficult to selectivity stack the only arteriole and capillary vessels which rink to cancer cells. However, blood fluidic condition is very complicated, and catheter's position, amount of anticancer drug and gelatin sponge, fluidic and pressure condition, environmental condition changed by catheter and effects to other

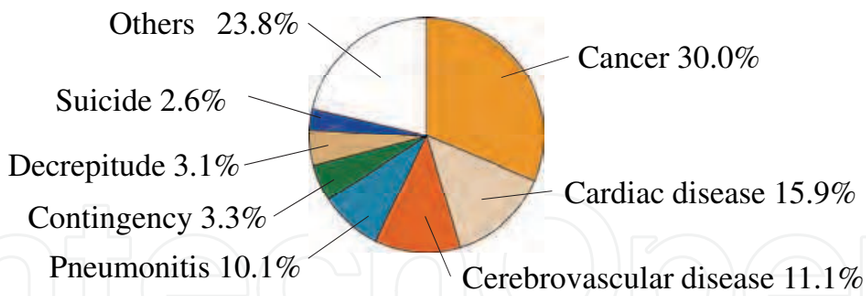


Fig. 1.1 The causes of the death in Japan in 2008.

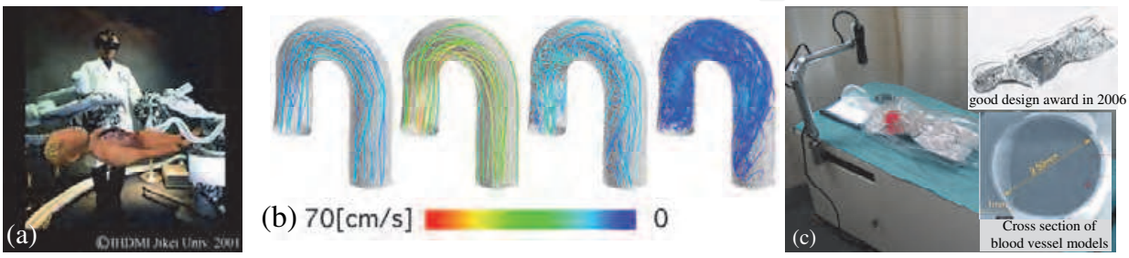


Fig. 1.2 Conventional surgical simulators. (a) VR surgical simulator (The Jikei Univ.). (b) Streamlines of blood flow by CFD analysis (Yamaguchi Lab. In Tohoku Univ.). (c) Our surgical simulator (Endo Vascular Evaluator: EVE).

tissue are unknown. DDS method protocol is similar to TAE, it is needed to discuss about optimizing applied dose, amount of diffusion of medicine and circulatory effect. On these accounts, the inspection based on detail plan and preparations experiment is necessary before performing real operations. And, the system for resolving these necessaries is required. For realizing a system of evaluating new treatment method using narrow vessels, we proposed circulation type blood vessel simulator (Fig.1.4). And, circulation type blood vessel simulator is needed to have artery models, narrow blood vessel models (arteriole and capillary vessel models) and vein models. In treatment of blood vessel diseases, medical doctors perform blood vessel shape maintenance with stent after a disease department was treated with a catheter for vascular disease treatment by manual skill. For practicing this manual skill, circulation type simulators having arteriole and capillary vessel models are required. Various studies are reported as surgical simulators and processing techniques of microchannels to arteriole and capillary vessel models. However, as for the conventional studies, narrow vessel models are not built into the systems, and a cross section of microchannels is near to a quadrangle. Therefore, they cannot realize human circulatory organ systems and blood vessels environments. In this chapter, realizing circulation type blood vessel simulators and producing arteriole and capillary vessel models having a circular cross section are aimed at.

Surgical simulators are used in practice and rehearsal for intravascular neurosurgery, and for development of new medical instruments such as catheters. Human carotid artery was made by combining processes of ink jet rapid prototyping, lost wax, dip coating, and selective dissolution. 3D configuration of carotid artery is developed by our 3D reconstructive method as described previously. These blood vessel models are made only for the artery, but reproduce the softness of a real blood vessel by controlling a film

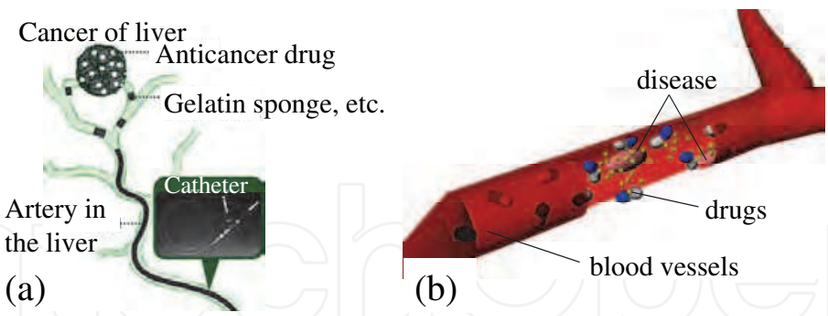


Fig. 1.3 Image of new treatment methods using narrow vessels. (a) Trancecatheter arterial chemoembolization (TACE, TAE). (The Japanese Society of Interventional Radiology, http://www.jsair.org/). (b) Drug delivery system (DDS).

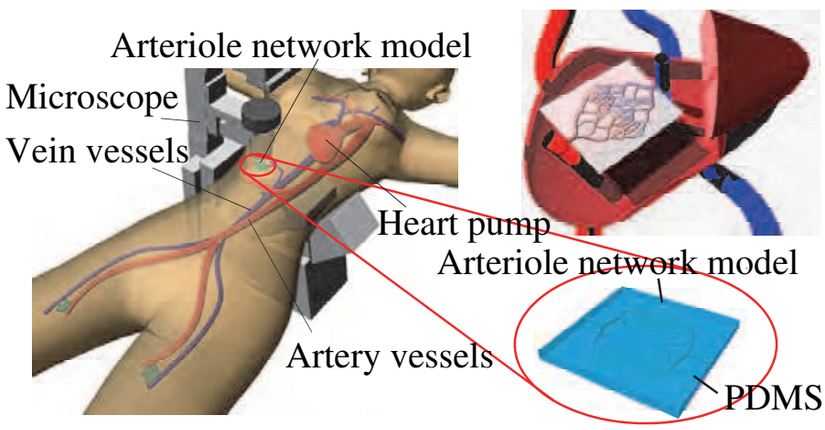


Fig. 1.4 Proposed circulation type blood vessel simulator.

thickness by dip lotion coating. Then, we developed a transparent surgical simulator by connecting the elastic tube models. Wax models are made by layer stacked modeling machine, however, the narrowest model's diameter is 500 um due to its low resolution and the brittleness of the wax. Therefore, a simulator cannot make a blood vessel model of narrower than 500 um inside diameter. Diseases exist in blood vessels such as arteria basilaris that are narrower than 500 um. Narrower blood vessel models are needed to simulate a more realistic vessel environment as shown in Fig.1.4. Previous surgical simulators are not suitable for rehearsal and training for such diseases.

The latest treatments for cancer and blood vessel disease from blood vessels are researched, but the evaluations and rehearsals are demonstrated with animal bodies. These evaluations and rehearsals should be demonstrated with the blood vessel simulator which is mimicked real blood vessel structures of human body. Therefore, it is very important to make a blood vessel simulator mimicking the human body. Flexibility of our previous blood vessel models have no problem, but cannot know influence in an end blood vessel of treatment because a blood vessel model is larger than 500 um inside diameter. Therefore, the arteriole and capillary vessel models were needed as a simulator to know influence in an end blood vessel. This study is targeted to fabricate multiscale transparent 10–500 um diameter arteriole and capillary vessel models that enable easy simulation of blood circulations. In

addition, fabricated microvessel models are needed to over the arteria pulmonalis's circularity which is 52.4%, and the circularity of microchannels is calculated by the shortest axis divided by the longest axis (Attinger, 1964). For this purpose, fabricated 10–500 um microvessel models must be circular cross sections, and circularities must be higher than 52.4%. In fact, a real blood vessel system has blood vessels of artery system and vein system. The targeted inside diameter of the blood vessel is 10-500 um (Hayashi, 1997). When microvessel models simulating real blood vessel are made, fabrication techniques should have high resolution processing about around 1 um (Noda et al., 2007; Itoga et al., 2004). Therefore, maicrofabrication processing technique is suitable for this requirement (Borenstein et al., 2002).

Many methods such as machining, stereolithography, ink jet rapid prototyping, and photolithography have been proposed for fabricating microchannels. Machining is suitable for a straight channel up to around 10 um in diameter, but not for complicated capillary vessel networks. Stereolithography is applicable for fabricating a mold; however, it is difficult to dissolve it to create a hollow structure. Ink jet rapid prototyping is beneficial for thicker tube channels such as aortas, but not applicable for capillary vessel models. Photolithography is a fundamental technology for fabricating microchannels, and a high resolution around 1 um is easily attained. We have chosen photolithography for fabricating microvessel models. In general, fabricating microchannels with a circular cross section is quite complex (Hanai et al., 2005; Eisner & Schwider, 1996; Nicolas et al., 1998). Microchannels were fabricated by using diffused-light, reactive ion etch (RIE) lag, and light curable resin, but the cross sections of the fabricated microchannels were semicircular, large diameter and not fine surface (Futai et al., 2004). These processes are not suitable for fabricating fine and narrow diameter blood vessel models. Therefore, we proposed a new fabrication process for multiscale transparent arteriole and capillary vessel models. And, these models have circular cross section made by over exposure method, reflow method and grayscale lithography as photolithography process. The fabricated microvessel models were connected with conventional blood vessel models to realize a circulation simulator. For example, circulation models will allow simulation of animal testing and drug delivery systems by using microvessels. In this chapter, we report multiscale fabrication method of arteriole and capillary vessel models and prototyping results for the circulation models.

2. Block type multi scale arteriole and capillary vessel models

2.1 Fabrication method

Figure 2.1 shows multiscale fabrication methods of blood vessel models. We used layer stack molding machine and photolithography process such as over exposure method, reflow method, and grayscale lithography. Because of a limit of fabrication accuracy, it is necessary to choose an appropriate method to fabricate a model with targeted diameter. A 10-20 um diameter capillary vessel models are made by over exposure method, a 20-100 um diameter arteriole models are made by reflow method, and a 100-500 um diameter arteriole models are made by grayscale lithography. The fabricated patterns are transcribed onto poly(dimethylsiloxane) (PDMS) substrate (Wu et al., 2002; Whitesides et al., 2001). After these processes, each patterned surface of two patterned PDMS substrates are treated by plasma and heated (Fig.2.2). Then, arteriole and capillary vessel models with circular cross section are completed (Arai et al., 2007).

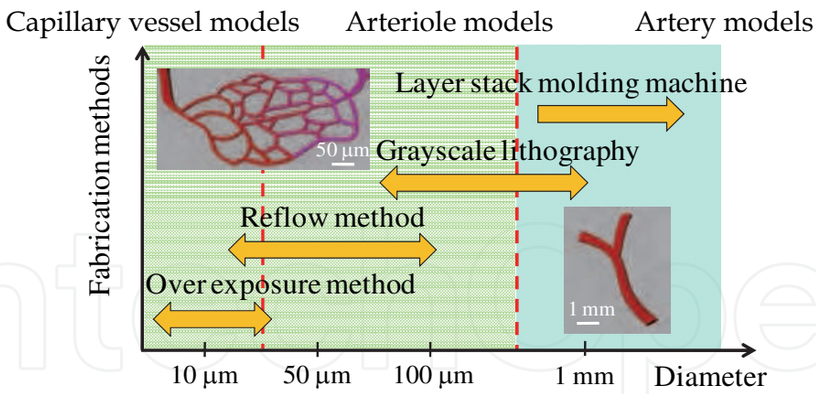


Fig. 2.1. Concept of fabrication methods for multi scale blood vessel models.

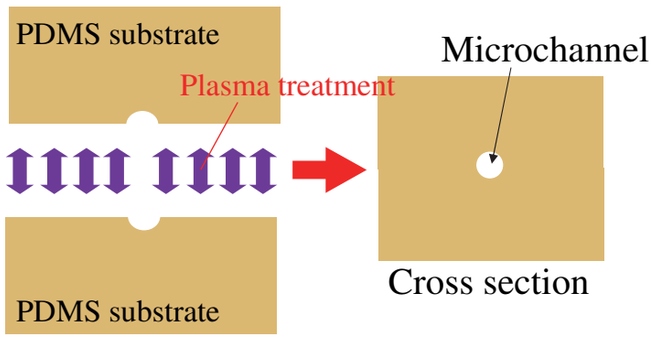


Fig. 2.2 Concept of making arteriole and capillary vessel model.

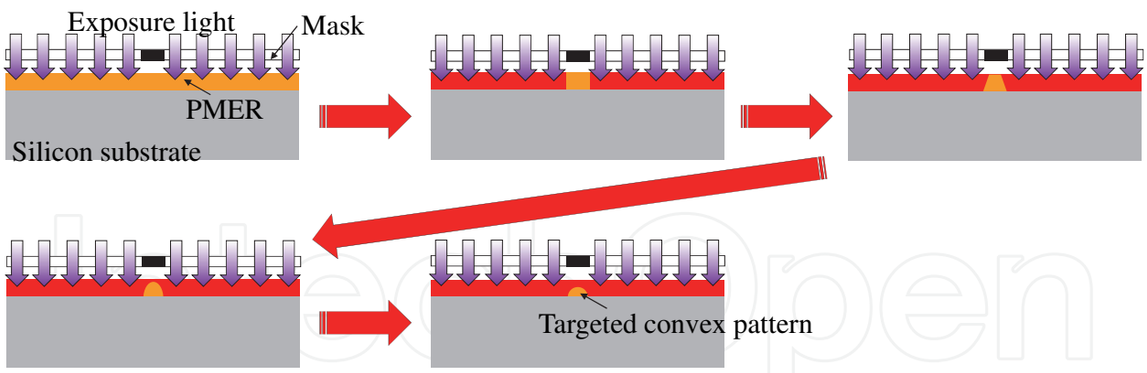


Fig. 2.3 The mechanism of over exposure method using diffracted light.

2.1.1 Fabrication of 10-20 um capillary vessel models

Fabrication method of capillary vessel models is over exposure method. In this exposure method, it is most important to expose at soft-contact using a mask and a resist surface. The soft-contact distance between the mask and a resist surface is 10-20 um. Exposure light is diffracted by the mask patterns. Exposed resist pattern can have the semicircular cross section by diffracted light. Figure 2.3 shows the mechanism of over exposure method for fabricating semicircular cross section patterns. In this process, a photoresist is PMER P-LA900PM (recommended exposure amount: 800-1200 Doses) as posi-type photoresist.

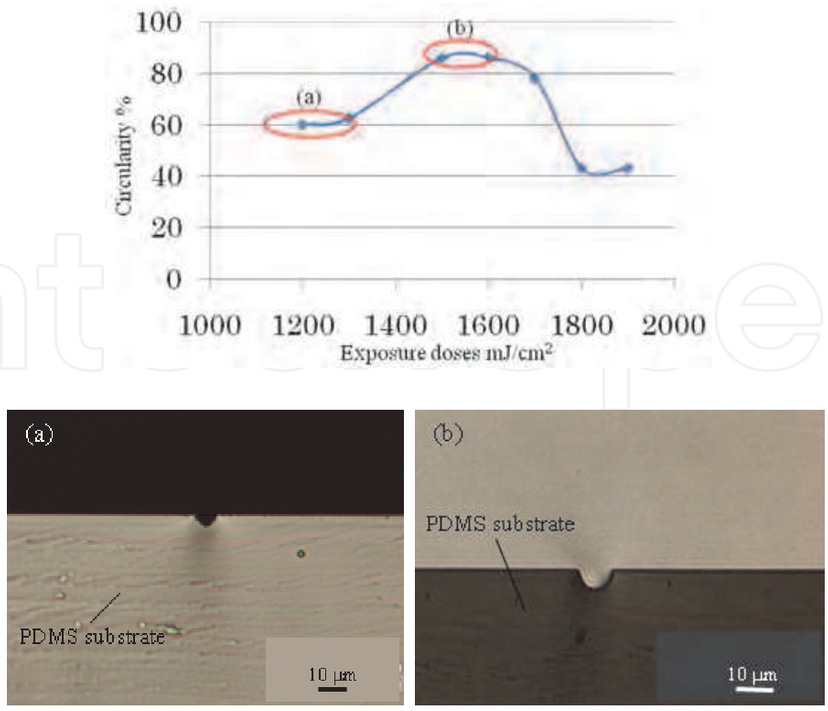


Fig. 2.4 Circularity result at each exposed dose. (a) shows the shape of microchannel in 1200-1400 doses. (b) shows the shape of microchannel in 1500-1700 doses.

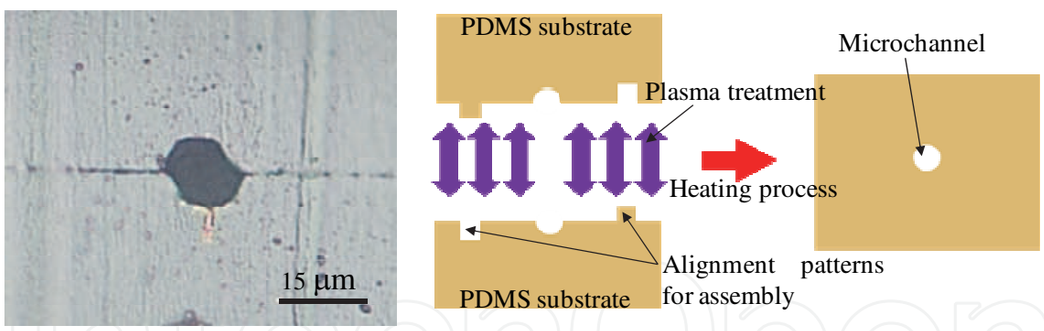


Fig. 2.5 Cross section of fabricated model, and new fabrication concept.

PMER is very sensitive resist for exposure light. Within the definite range of recommended exposure amount, the cross section of resist patterns is square. The cross section shape of resist patterns is varying trapezoid, triangular, semiround and oval by increasing the exposure light amount. Therefore, exposure light amount (exposure doses) should be controlled. And, we experimented and calculated relation between circularity and exposure doses. Figure 2.4 shows circularity result at each exposed dose. In 1200-1400 doses, the cross section of resist pattern shape is the trapezoid or triangular, and the circularity is low with about 60%. In 1500-1700 doses, the cross section of resist pattern shape is the semicircular, and the circularity is high with about 80%. In over 1700 doses, the resist pattern shape is the oval, and the circularity falls fast until about 40%. (a) shows the peak at triangular shape, lowers afterwards the height part, and receives (b) that is the peak value at round shape in

figure though are in the circularity two peak values of (a) and (b). The reason why the graph has increased and decreased is that the number of sampling to each light exposure was one time. Figure 2.5 shows cross section of fabricated capillary vessel models. When two PDMSsubstrates assemble, alignment is very difficult and patterns are out of alignment. To solve this problem, new patterns are needed for PDMS substrates assembly (Fig.2.5). And, new capillary vessel pattern and assembly pattern are fabricated by multi stage exposure photolithography. The fabrication process is following:

A. Fabrication of patterns for alignment

1. Coat a substrate with 8-um-thick photoresist PMER.
2. Expose at hard-contact using both a mask and a resist surface until 1000 Doses.
3. Develop for 7 minutes.
4. Hardbake at 145°C for 30min.

B. Fabrication of other patterns for alignment

1. After using plasma hydrophilic treatment, coat a substrate with 8-um-thick PMER.
2. Expose at hard-contact using both a mask and a resist surface until 1000 Doses.
3. Develop for 7 minutes.
4. Hardbake at 145°C for 30min.

C. Fabrication of pattern for microchannels

1. After using plasma hydrophilic treatment, coat a substrate with 8-um-thick PMER.
2. Expose at soft-contact using both a mask and a resist surface until 1500 Doses.
3. Develop for 5 minutes.
4. Transcribe resist patterns onto PDMS.

And, the capillary vessel model was completed by bonding two patterned PDMS substrates.

2.3.2 Fabrication of 20-100 um arteriole models

Fabrication method of 20–100 um arteriole models is reflow method. In this fabrication method, it is most important to control the resist pattern's height. Then, the evaluation of the resist patterns' height in a longer direction is needed. The resist patterns' height fabricated by reflow method was measured 10 times at random parts at 1 mm certain interval by using prove. Table 2.1 shows the evaluation results. The differences of resist patterns' height were less than 1.5 um. And, real blood vessels have a rough surface which is few micrometers, and reflow method is suitable for fabricating 20–100 um arteriole models. In reflow method, resist thickness must be changed by each targeted diameter. The 20–100 um arteriole models were fabricated by using this calculated resist thickness (Not shown). Next, the fabrication process based on reflow method was explained. The fabrication process is following:

1. Coating photoresist PMER on silicon substrate.
2. Exposure until 1000 Doses.
3. Development for 7 minutes.
4. Heating the resist patterns from bottom side by hot plate at 145°C for 30-60 seconds.
5. Transcribing these resist patterns onto PDMS.

After the development, the resist pattern was heated from back side of silicon substrate. The patterned resists become liquid again in this process, and the semicircular resist pattern was fabricated by liquid surface tension. Then, the arteriole models were completed by bonding two patterned PDMS substrates.

Diameter [um]	Difference of patterns' height [um]
10	0.58
20	0.18
30	0.47
40	1.0
50	1.5

Table 2.1 Profiling results of the resist patterns' height

2.3.3 Fabrication of 100-500 um arteriole models

Fabrication method of 100–500 um arteriole models is grayscale lithography. In this fabrication method, it is most important to control histogram of grayscale mask (O'Shea & Rockward, 1995). In general, grayscale mask is very high cost. In this time, the grayscale emulsion mask is made by 1/20 reduction machine with imagesetter film (3600 dpi) due tolow cost and simple process fabrications (Fig.2.6). Because fabricated grayscale mask has 256 shades of gray, the resists' height made by UV lamp power through the each gray tone has difference. Therefore, calibration of relation between curable depth (capable of fabricate resist patterns' height) and UV lamp power (gray level) is required. Figure 2.7 shows the evaluation result. Using this result, the grayscale emulsion mask was designed and fabricated. Next, the fabrication process based on grayscale lithography was explained. The fabrication process is following:

1. Coating naga-photoresist SU-8 on glass substrate.
2. Illuminating from the back side of substrate through grayscale emulsion mask.
3. Development to be 3D shape.
4. Transcribing these resist patterns onto PDMS.

And, the arteriole models were completed by bonding two patterned PDMS substrates.

2.4 Results and evaluations

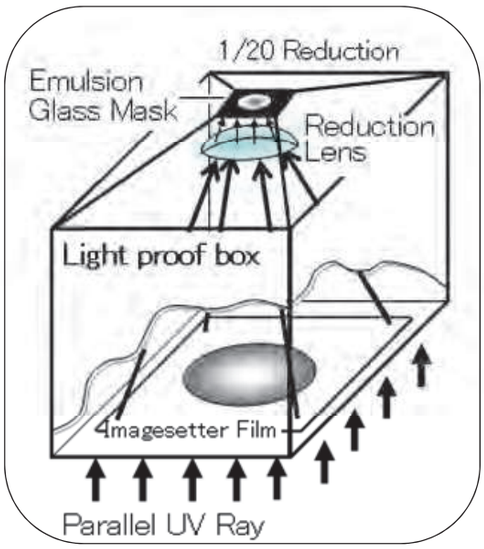
We evaluated the alignment accuracy of the capillary vessel models. A model having no alignment pattern had an alignment error of 2.5 um, whereas, a model with alignment patterns had an alignment error of 0.6 um. The circularity of the capillary vessel model having no alignment pattern was 70% and for that with alignment patterns was 84%. Thus, alignment patterns reduced the alignment error from 2.5 to 0.6 um and improved the circularity from 70 to 84%. Figure 2.8 shows the cross sections of fabricated arteriole and capillary vessel models. In addition, the circularity of 10 um microchannel is 84.0%, that of 50 um microchannel is 61.5%, and that of 500 um microchannel is 82.3%.

3. Tube type arteriole models

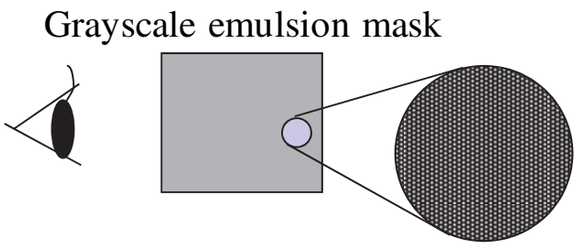
3.1 Evaluation of wax + polyvinyl alcohol (PVA) mixture material

We completed block type microvessel models by using photolithography in section 2. However, block models cannot recreate moderate compliance which is similar to that of the real blood vessel. To solve this problem, arteriole and capillary vessel tube models are needed for surgical simulator. And, sacrificial models are needed to make tube models. But because of brittleness of wax, under 500 um diameter sacrificial models cannot be made by using layer stack molding machine. In this section, a novel fabrication method for transparent arteriole tube models is proposed. Improving the brittleness of wax by mixing

wax with PVA was tried. After making sacrificial models made of mixture material, arteriole tube models were completed by dip coating.



(a) Concept of 1/20 Reduction System.



(b) Image of fabricated grayscale emulsion mask.

Fig. 2.6 Fabrication concept of grayscale emulsion mask.

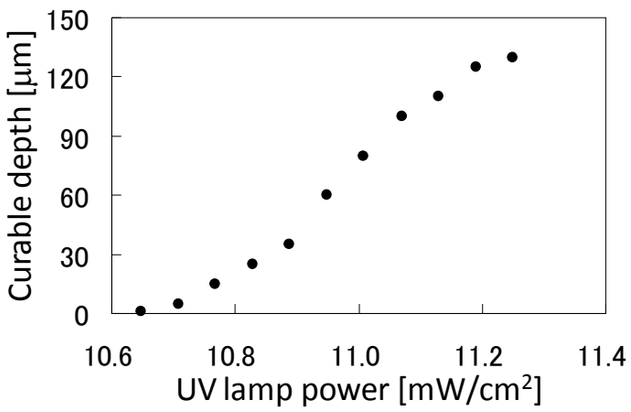


Fig. 2.7 Calibration of relation between curable depth (capable of fabricate resist patterns' height) and UV lamp power (gray level).

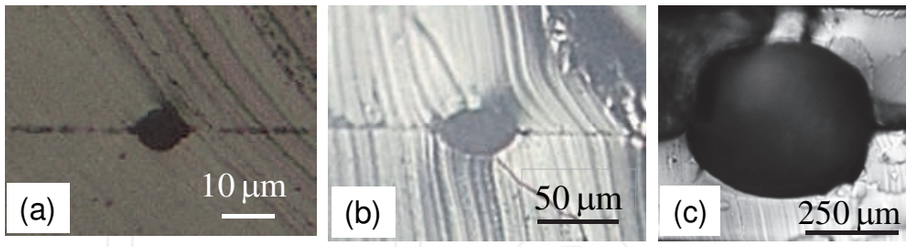


Fig. 2.8 Cross sections of fabricated models. (a) 10 um (b) 50 um (c) 500 um

In this fabrication process, wax and PVA mixture material is used to build sacrificial models. These models are very useful for fabricating tube models narrower than 500 um. If only wax is used for making sacrificial models, the temperature is needed to keep. And wax is not suitable to this fabrication process because of wax's fragility. If only PVA is used for making sacrificial models, PVA model is deformed easily by model's own weight when dip coating, since it has low bend strength. Therefore, the new method of fabricating sacrificial models was proposed with wax and PVA mixture materials. The mixture has the properties of both wax and PVA can be easily forecasted. The properties of mixture were evaluated by changing the mix ratio. Evaluated properties are Young's modulus as mechanical property and melting materials times in different liquid (solubility) as chemical property. Evaluated samples made by different mix ratio (mix ratio wax: PVA= 1:0, 1:4, 2:3, 3:2, 4:1, 0:1).

Tensile tester is used for evaluation experiments of Young's modulus. Samples made by wax and PVA mixture materials are made 50 mm × 10 mm × 2 mm (long × wide × thick) in size. The tensile experiment was demonstrated three times for each wax and PVA mix ratio. Using these results, the Young's modulus was calculated. Young's modulus of each mix ratio is calculated by averaging the experimental results. Table 3.1 shows Young's modulus by each mix ratio. Young's modulus of PVA is 9.57 MPa. On the other hand, Young's modulus of wax is 20.6 MPa. As you can see, Young's modulus of mixture material is getting higher by increasing the ratio of wax. And also, Table 3.1 shows extension. Extension is expression of material's brittleness and ductibility. Extension of mixture material is getting higher by increasing the ration of PVA. Therefore, the mechanical property of wax and PVA mixture material can be controlled by changing mix ratio.

Next, melting time of each different ratio mixture materials was measured in different liquid by checking mass changes. The solubility of each mix ratio was defined from experiment. Using ultrasound bath was set at 50°C for solubility experiments. Deionized water (DI water), acetone, and DI water + acetone liquid mixture were provided for this test. DI water easily melts PVA. Acetone easily melts wax. Liquid mixture of 1:1 mix ratio was provided, since melting samples was wax and PVA mixture material. The liquid was used in the melting experiments. Figure 3.1 shows the experimental results about observing solubility of each sample in DI water, acetone, DI water and acetone liquid mixture. Because of DI water's feature, mixture material samples were melted easily. In this result, mass changes of the wax sample were observed. This is caused by heating in the process of ultrasound bath and etching effects. Acetone melted few mixture material was observed in this experiment, although acetone can melt wax easily. It happened since wax was coated with PVA, and acetone could not reach wax. On the other hand, mixture material was melted by liquid mixture. That was verified by experiment. Comparing these results, all mixture materials cloud be melted in DI water and acetone liquid mixture, however, dissolving rate was decreasing. PVA absorbed DI water and increased mass was observed when experiments

started. These results suggested DI water and acetone liquid mixture is suitable for melting the wax and PVA mixture materials.

PVA: wax ratio[%]	Young's modulus [MPa]	Extension [%]
1:0	9.57	75
4:1	9.69	75
3:2	8.78	75
2:3	15.7	44
1:4	22.8	4.0
0:1	20.6	6.0

Table 3.1. Experimental rigidity and extension

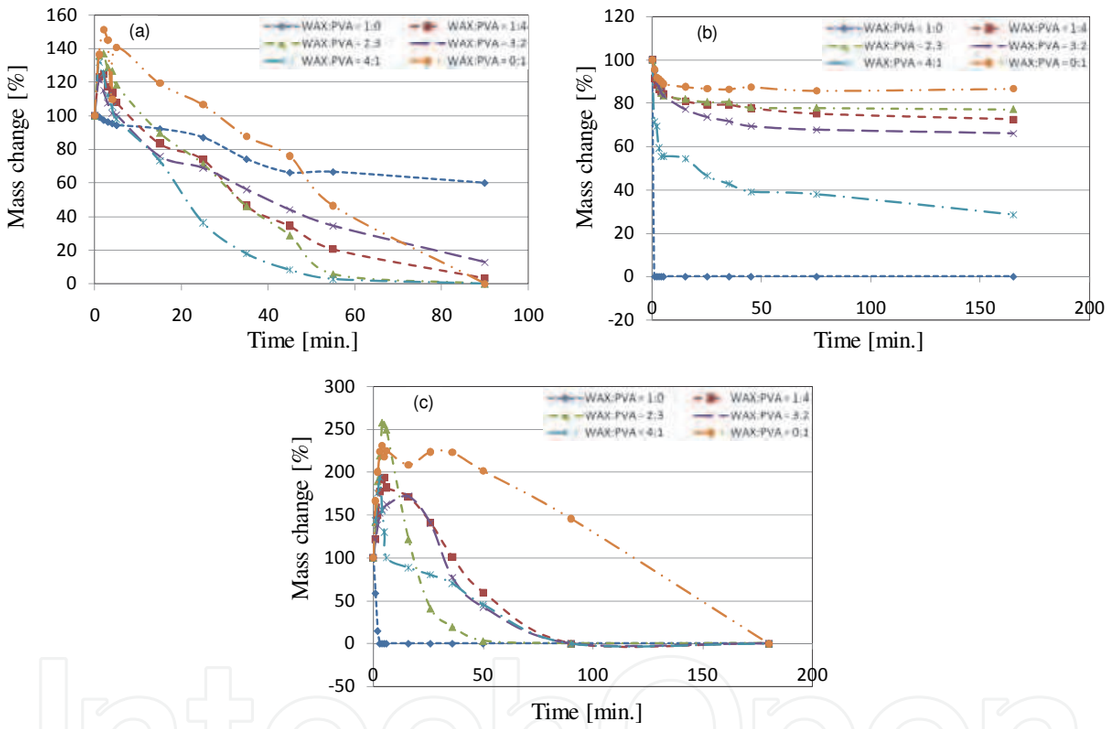


Fig. 3.1 Evaluation of chemical features. (a) DI water (b) Acetone (c) Acetone + DI water

3.2 Fabrication of arteriole tube models

For fabricating arteriole tube models, sacrificial models as molds for dip coating of PVA and silicone resin are needed. The sacrificial models with this wax and PVA mixture were fabricated. Patterned PDMS substrates for molding sacrificial models were made by explained method in section 2. Fabrication process flow for sacrificial models is following:

1. Coating wax and PVA mixture materials on patterned side of PDMS substrate.
2. Splitting and removing superfluous mixture.
3. Aligning two patterned PDMS substrates filled with mixture on patterned side.
4. After drying at room temperature, removing the PDMS substrates.
5. Removing mixture stacking on the sacrificial models.

Figure 3.2 shows the sacrificial model before and after removing stacking mixture on model surface. The stacking mixture was cut and etched with DI water. And, Fig.3.2(b) shows the cleared and smoothed surface on sacrificial model. Then, we fabricated arteriole tube models by using the sacrificial models. This sacrificial model was coated with PVA for smoothing the surface and later coated with transparent silicone resin for tube structure by dip coating based on previous method. After dip coating, sacrificial model and PVA for smoothing were dissolved by DI water and acetone, and transparent arteriole tube models were completed. Fabrication process flow is following:

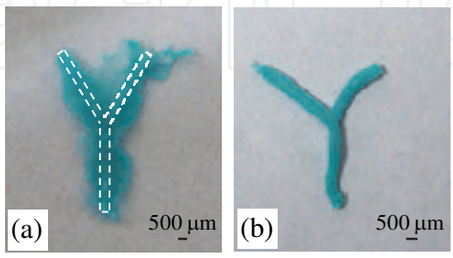


Fig. 3.2 Fabricated sacrificial models. (a) The before removing. (b) The after removing.

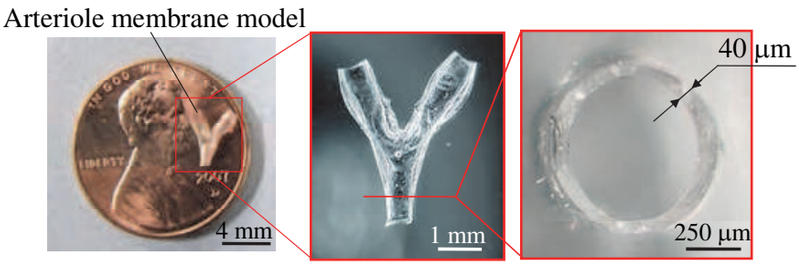


Fig. 3.3 Fabricated arteriole tube model. (a) Fabricated model. (b) Overall. (c) Cross section.

1. Dip coating the sacrificial models with 10wt% PVA solution for smoothing the surface.
2. After drying, dip coating the PVA coated sacrificial models with silicone resin.
3. Dissolving sacrificial models and PVA layer by DI water and acetone liquid mixture.
4. Drying silicone tube structures and completing blood vessel tube models.

Figure 3.3 shows fabricated arteriole tube model. The tube and hollow structures were observed. And, fabricated arteriole tube model had circular cross section shown in Fig.3.3(b). The calculated circularity of this model was 90%. As you can see, the thickness of fabricated model was not uniform. The thickest part is 350 um. Changing the ratio of base resin and curing agent consisted of silicone resin can decrease viscosity, then, coat uniform.

4. Network type arteriole models

4.1 Design of network structure

Our fabricated arteriole and capillary vessel models are transparent and Y shape branched microchannels, but diameters are uniform around branched structure. These models cannot recreate the real blood vessel environments. To solve this problem, microvessel models based on real blood vessel branched rule is proposed and fabricated. This rule is based on the cube law between mother blood vessel's diameter and daughter blood vessels' diameters. Real blood vessel is branched structure based on the cube law shown in Fig.4.1. Therefore, the network branched microchannels were designed by using this rule. The

microchannels are changed diameters when these are branched. The rule of changing diameter is shown in equation (1).

$$R_0^3 = R_1^3 + R_2^3 \quad (1)$$

In Eq. 1, R_0 is mother blood vessel's diameter. R_1 and R_2 are daughter blood vessels' diameters (Sherman, 1981).

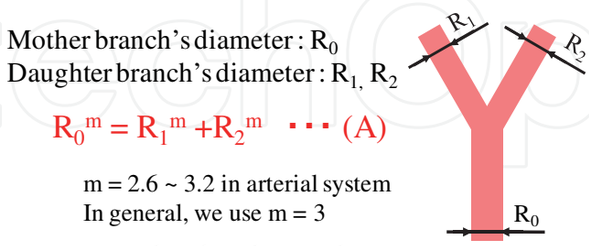


Fig. 4.1 The branched structure rule of real vascular.

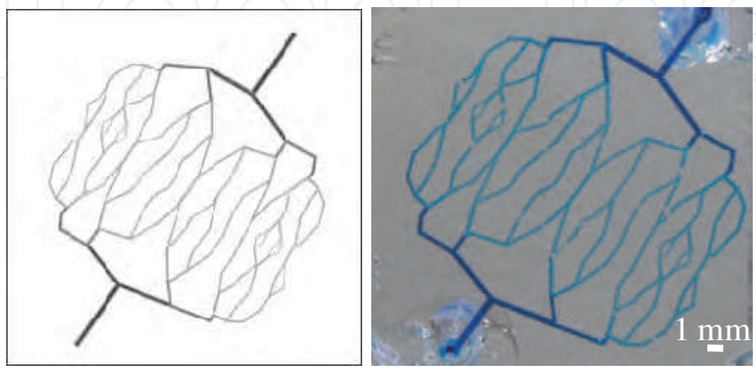
4.2 Fabrication and evaluation

4.2.1 100-500 um network type arteriole models

Table 4.1 shows the parameters of blood vessel models' diameters using this rule. Using these parameters, grayscale mask was designed (Fig.4.2(a)). And, the 100–500 um arteriole network models were fabricated by grayscale lithography and PDMS bonding. The fabrication process is following.

Daughter diameters		Mother diameters
R_1 [um]	R_2 [um]	R_0 [um]
100	100	126
126	126	159
159	159	200
200	200	252
252	252	317
317	317	400
400	400	504

Table 4.1 Calculated the diameter parameter based on the rule (100–500 um).



(a) Designed grayscale mask. (b) Fabricated model.

Fig. 4.2 100-500 um diameter network type arteriole models.

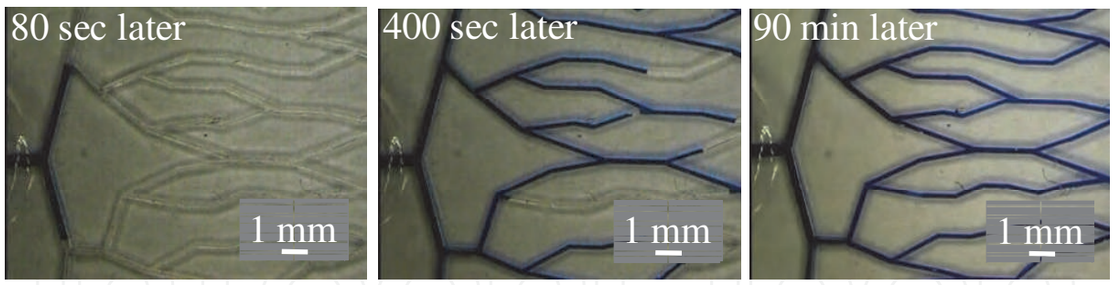


Fig. 4.3 The results of flow evaluation.

1. Coating nega-photoresist on glass substrate.
2. Exposing from the back side of substrate through grayscale mask.
3. Developing photoresist patterns to be 3D shape.
4. Transcribing these patterns onto PDMS substrate.
5. Bonding the two PDMS substrates by plasma treatment and heating.

Completed model was shown in Fig.4.2(b). Figure 4.3 shows the fluid evaluation using fabricated arteriole model which had 100–500 um diameter. A flow condition was 1 ul/min. This fabricated model had no leakage, and was observed different flow speed in same diameter microchannel. It is because that branched angle may effect to flow speed and pressure.

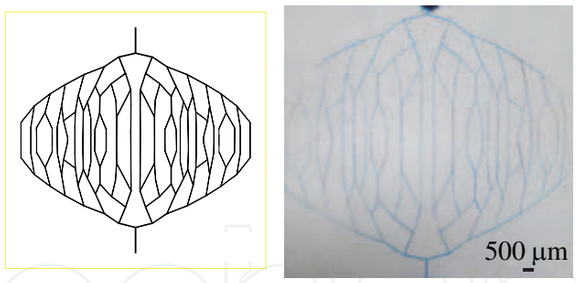
4.2.2 20-100 um network type arteriole models

Using Eq. 1, diameter parameter was calculated for fabricating 20–100 um network type arteriole models. Table 4.2 shows the calculated parameters of arteriole network models based on the cube law. The mask for fabricating 20–100 um network type arteriole models was designed(Fig.4.4(a)). In reflow process, it is important to control the photoresist thickness. In this time, thickness of coated resist was 16 um, because reflowed resist tend to flow from narrow diameter to large diameter. Then, the 20–100 um arteriole network models were fabricated by reflow method and PDMS bonding. The fabrication process is following.

1. Coating photoresist PMER on silicon substrate.
2. Exposure until 1000 Doses.
3. Development for 7 minutes.
4. Heating the resist patterns from bottom side by hot plate at 145°C for 30-60 seconds.
5. Transcribing these resist patterns onto PDMS.

Daughter diameter		Mother diameter
R_1 [um]	R_2 [um]	R_0 [um]
19.8	19.8	25.0
25.0	25.0	31.5
31.5	31.5	39.7
39.7	39.7	50.0
50.0	50.0	63.0
63,0	63.0	79.4
79.4	79.4	100

Table 4.2 Calculated the diameter parameter based on the rule (20–100 um).



(a) Designed mask data (b) Fabricated model.

Fig. 4.4 20-100 um diameter network type arteriole models.

Fabricated network model was shown in Fig.4.4(b). It was confirmed fabricated microchannels had no leakage by flow test.

5. Circulation type blood vessel simulators

5.1 Fabrication by seamless connecting

Our artery and network arteriole models are made by the different processes, therefore, seamless connection is the key issue. Then, our concept of fabricating circulation models was proposed in Fig.5.1. In this method, the circulation model was fabricated by seamless connecting arteriole network models and artery models (whose smallest blood vessel model is 5.0 mm diameter) with connector models made of wax.

In seamless connecting method, wax connector models were used for connecting the 500 um microchannel of the arteriole network and the 5.0 mm macrochannel. The designed wax connector model is shown in Fig.5.2 (a) and (b). This connector was fabricated by ink jet rapid prototyping, and had shafts for aligning the central axis of each channel. A 500 um shaft was needed to insert in the network model channel and a 0.8 mm shaft was needed to insert wax models in the artery model. The wax model of the artery had a 1.0 mm hole for insertion and alignment as shown in Fig.5.2 (c). The connection process flow is following:

A. Connection process for the network model (Fig.5.3)

1. Dip coating the wax connector with PVA to smoothen the surface.
2. Inserting the connector in the network model, and temporarily fixing with PDMS.
3. Completely fixing with PDMS.

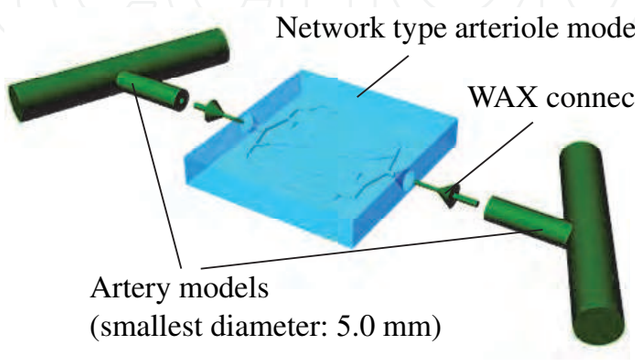


Fig. 5.1 Concept of fabricating circulation models for seamless connection.



(a) Designed connector (b) Fabricated connector (c) artery wax model

Fig. 5.2 Wax connectors and connection hole of artery wax model.

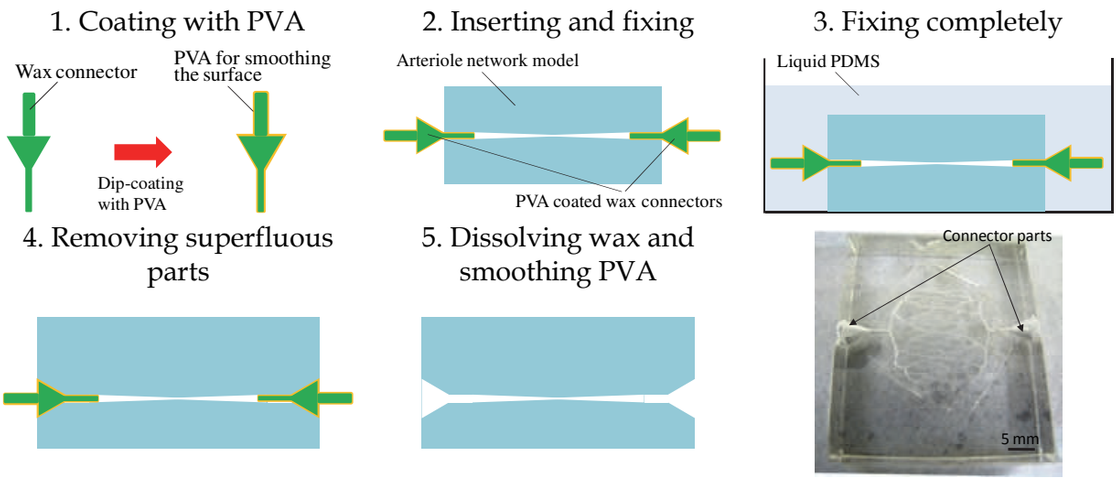


Fig. 5.3 Connection process for the network model.

4. Removing superfluous PDMS mold.
5. Dissolving the wax and smoothing PVA.

B. Connection process for an artery model (Fig.5.4)

1. Smoothing the surface of the wax artery model by dip coating with PVA.
2. Dip coating with silicone resin.
3. Removing the silicone resin and PVA from the alignment hole.
4. Inserting the 0.8 mm shaft of a PVA coated connector in the alignment hole.
5. Fixing the wax connector on the alignment hole with PVA.

These models were connected to make a circulation model. For fixing, the connector parts were coated with silicone resin, adjusted relative to each other, and heated at 55°C for an hour. This assembly process produced the circulation model. Figure 5.5 shows the fabrication process, and fabricated circulation blood vessel model.

5.2 Evaluation with fabricated circulation model

For evaluation of leakage check, we performed flow experiments with the fabricated circulation model using a methylene blue solution. The flow rate was 1 ul/min, (This flow rate was 0.016 mm/s in the 500 um in diameter microchannel.) and the experiment demonstrated that these channels had no leakage. We also confirmed that the methylene blue solution flowed from the inlet to the outlet. The connected parts between the arteriole

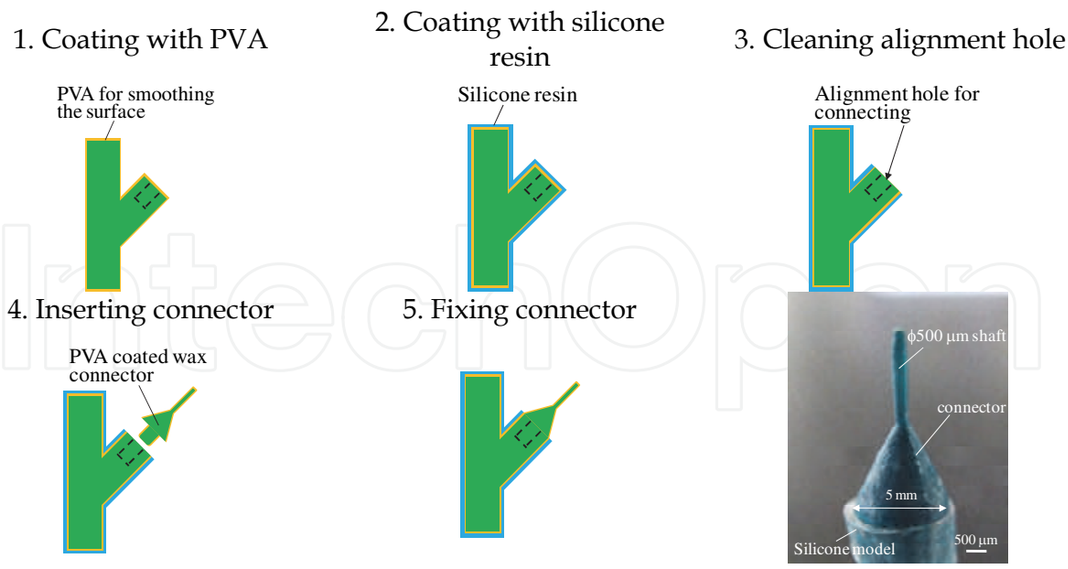


Fig. 5.4 Connection process for the artery model.

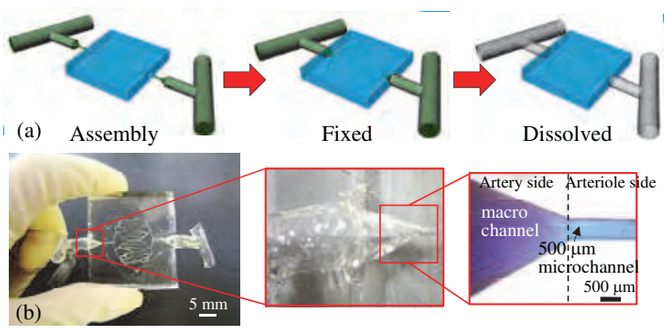


Fig. 5.5 Connection process for the artery model.

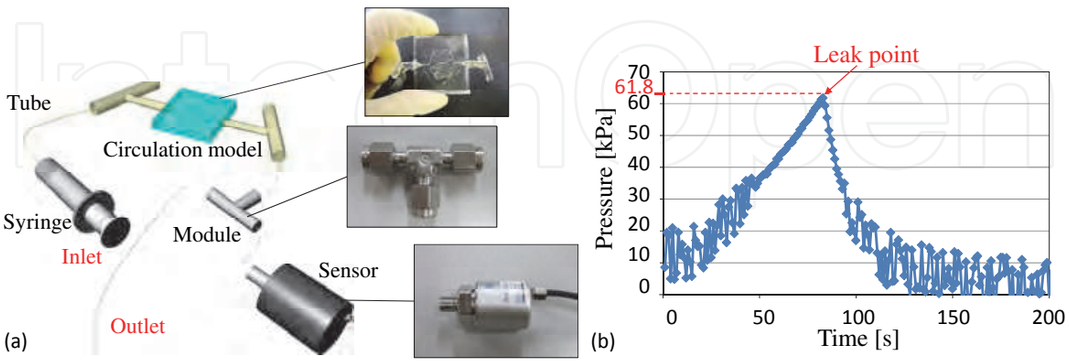


Fig. 5.6 Pressure test with fabricated model. (a)Setup for experiment. (b)Experimental result.

network model and artery models exhibited no leakage. The proposed method was suitable for fabricating circulation models. Next, a pressure test was conducted using the fabricated circulation model. Figure 5.6(a) shows the pressure test setup. The prepared pressure sensor

can measure the liquid pressure. First, the microchannels of the circulation model were filled with DI water. The outlet part was sealed off in order to increase the pressure inside the circulation model by the syringe pump. The experimental results revealed that the leak pressure was approximately 61.8 kPa as shown in Fig.5.6(b). The leak point was located on the artery model. The pressure resistance of the fabricated circulation model was confirmed to be larger than the pressure of actual blood vessels. For example, the pressure in the artery is 16 kPa, and that in the arteriole is 13 kPa (Whitmore, 1968). Therefore, the results of the pressure test using the fabricated circulation model show our model is capable of withstanding the pressures of real blood flow. Next, the pressure loss across the inlet and outlet of the fabricated circulation model was measured. This experiment required the use of two pressure sensors. One sensor was used to measure the pressure at the inlet side, and the other sensor was used to measure the pressure at the outlet side. The pressure loss was obtained by subtracting the pressure measured at the outlet side from the pressure measured at the inlet side. The pressure measured at the inlet side was 9.43 kPa, and that measured at the outlet side was 9.18 kPa. Thus, the pressure loss was 250 Pa. This pressure loss may be caused by a high friction coefficient of silicone resin and PDMS and the length and structure of the channels. This pressure loss was sufficiently small.

6. Conclusion

This chapter reported four research topics that can be categorized into following two areas; (i) Various types of microvessel models for blood vessel simulator (Section 2, 3, 4), (ii) Seamless connecting for realizing circulation type blood vessel simulator (Section 5).

In section 1, we introduced the background of conventional surgical simulators, and explained the needs of arteriole and capillary vessel models as surgical simulator for higher precision simulating. For fabricating these models, photolithography process was selected in many maicrofabrications.

In section 2, multiscale fabrication method of 10-500 um arteriole and capillary vessel models was proposed and demonstrated. It is necessary to choose an appropriate exposure method. From the experimental results, it was confirmed proposed method is useful for making microvessel models. These models were fabricated by photolithography and plasma bonding with patterned PDMS substrates. In fabricating capillary vessel models, when two PDMS substrates assembled, alignment is very difficult and patterns are out of alignment. Then, we proposed a novel assembly method. The method is fabricating capillary vessel model pattern and assembly pattern by multi stage exposure. And, the alignment accuracy of the capillary vessel models was evaluated. Then, the circularity of fabricated microchannels was calculated. Fabricated microchannels were 10 um diameter capillary vessel model, 50 um and 500 um diameter arteriole models. The circularity of 10 um microchannel is 84.0%, that of 50 um microchannel is 61.5%, and that of 500 um microchannel is 82.3%. All cross sections of microchannels were circular or elliptical.

In section 3, new fabrication method of 100-500 um arteriole tube models for surgical simulator was proposed. And, fabrication method of arteriole tube model and evaluation of the molding material (wax and PVA mixture material) were reported. For making tube model having narrower than 500 um, it is very important to use wax and PVA mixture material. And, mechanical and chemical properties of wax and PVA mixture material were evaluated. From evolutional results, the brittleness of the previous sacrificial model was

overcome by based on the proposed approach. And, we succeeded in making the tube and hollow structural arteriole model. This arteriole tube model had circular cross section inside the channel, and circularity of this channel was 90%.

In section 4, 100–500 um transparent arteriole network model was successfully fabricated. And, fabricated microchannels had no leakage by the flow experiment. Therefore, using grayscale lithography and basing on real vessels' branched rule are useful to fabricate 100–500 um transparent networked arteriole models. In addition, 20–100 um arteriole network model was successfully fabricated, too. The reflowed resist flowed from narrow diameter to large diameter. Therefore, comparing theoretical and experimental circularity, experimental circularity was dramatically improved. Then, reflow method is suitable for fabricating 20–100 um arteriole network models.

In section 5, circulation type blood vessel models were fabricated and demonstrated by using arteriole network models and artery models. A circulation model was fabricated using a wax connector for seamless connecting. The fabricated model had a seamless structure, and it was demonstrated by the flow experiments that this model had no leakage on the any parts. The proposed connection method was suitable for fabricating circulation models. And, fabricated circulation model can be used for blood vessel simulator from the result of pressure test. Therefore, the fabricated circulation model will be used to evaluate drug delivery systems, diacrisis, and medical treatments by ultrasound.

7. Acknowledgements

The present study was supported by a Grant-in-Aid for Scientific Research from the Ministry of Education, Culture, Sports, Science, and Technology of Japan and the Japan Society for the Promotion of Science (Grant Nos. 17076015, 18206027, and 214059).

8. References

Ikeda, S., Arai, F., Fukuda, T., Negoro, M., Irie, K. (2005). An In Vitro Patient-Tailored Biological Model of Cerebral Artery Reproduced with Membranous Configuration for Simulating Endovascular Intervention. *Journal of Robotics and Mechatronics,* Vol.17, No.3, June 2005, pp. 327-334, ISSN0915-3942 (print), 1883-8049 (online)

Attinger, E.O. (1964). *Pulsatile Blood Flow.*, Mc.Graw-Hill Book Co., New York, USA

Hayashi, K. (April 1997). *Biomechanical Engineering: A First Course*, MARUZEN CO., LTD., ISBN 4-88898-081-0, Tokyo, Japan

Noda, D., Matsumoto, Y., Setomoto, M. (2007). Fabrication of Coil Lines with High Aspect Ratio for Electromagnetic Actuators. *Proceedings of International Symposium on Micro-Nano Mechatronics and Human Science*, pp.436-441, Nagoya, Japan, date, 2007

Itoga, K., Yamato, M., Kobayashi, J., Kikuchi, A., Okano, T. (2004). Cell micropatterning using photopolymerization with a liquid crystal device commercial projector. *Biomaterials,* Vol.25, No.11, May 2004, pp.2047-2053, ISSN 0142-9612

Borenstein, J., T., Terai, H., King, K., R., Weinberg, E., J., Kaazempur-Mofrad, M., R., Vacanti, J., P. (2002), Microfabrication Technology for Vascularized Tissue Engineering. *Biomedical Microdevices*, Vol.4, No.3, July 2002, pp.167-175, ISSN 1387-2176 (Print) 1572-8781 (Online)

Hanai, K., Shimizu, S., Matsumoto, Y. (2005). Three Dimensional Structures of Negative-tone Photoresist by Binary Optics. *IEEJ Trans. SM*, Vol.125, No.10, January 2006, pp.424-425, ISSN 1341-8939 (print), 1347-5525 (online)

Eisner, M., Schwider, J. (1996). Transferring resist microlenses into silicon by reactive ion etching. *Opt. Eng.*, Vol.35, No.10, October 1996, pp.2979-2982, ISSN 0091-3286, 1560-2303 (eISSN)

Nicolas, S., Dufour-Gergam, E., Bosseboeuf, A., Bourouina, T., Gilles, J.-P., Grandchamp, J.-P. (1998). Fabrication of a gray-tone mask and pattern transfer in thick photoresists. *J. Micromech. Microeng.*, Vol.8, No.2, June 1998, pp.95-98, ISSN 0980-1317 (print), 1381-8439 (online)

Futai, N., Gu, W., Takayama, S. (2004). Rapid Prototyping of Microstructures with Bell-Shaped Cross-Sections and Its Application to Deformation-Based Microfluidic Valves. *Adv. Mater.,* Vol.16, No.15, August 2004, pp.1320-1323, ISSN 1521-4095

Wu, M-H., Park, C. & Whitesides, G. M. (2002). Fabrication of Arrays of Microlenses with Controlled Profiles Using Gray-Scale Microlens Projection Photolithography. *Langmuir*, Vol.18, No.24, November 2002, pp.9312-9318, ISSN 0743-7463 (print), 1520-5827 (online)

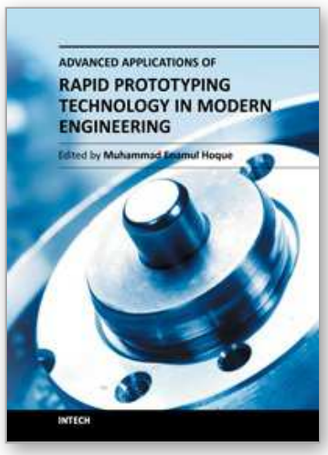
Whitesides, G. M., Ostuni, E., Takayama, S., Jiang, X., Ingber, D. E. (2001). Soft Lithography in Biology and Biochemistry. *Annu. Rev. Biomed. Eng.*, Vol.3, August 2001, pp.335-373

Arai, F., Nakano, T., Tada, M., Lin, Y.-C., Ikeda, S., Uchida, T., Oura, H., Fukuda, T., Matsuda, T., Negoro, M. (2007). Fabrication of cell-adhesion surface and Arteriole Model by photolithography. *Journal of Robotics and Mechatronics,* Vol.19, No.5, October 2007, pp.535-543, ISSN 0915-3942 (print), 1883-8049 (online)

O'Shea, C. & Rockward, W., S. (1995). Gray-scale masks for diffractive-optics fabrication: II. Spatially filtered halftone screens. *Appl. Opt.*, Vol.34, No.32, November 1995, pp.7518-7526, ISSN 1559-128X, 2155-3165 (eISSN)

Sherman, T., F. (1981). On Connecting Large Vessels to Small. The Meaning of Murray's Law. *J. Gen. Physiol.*, Vol.78, October 1981, pp.431-453, ISSN 0022-1295 (print), 1540-7748 (online)

Whitmore R. L. (1968). *Rheology of the Circulation*, Pergamon Press, ISBN 4-88898-081-0, Oxford, UK



Advanced Applications of Rapid Prototyping Technology in Modern Engineering

Edited by Dr. M. Hoque

ISBN 978-953-307-698-0
Hard cover, 364 pages
Publisher InTech
Published online 22, September, 2011
Published in print edition September, 2011

Rapid prototyping (RP) technology has been widely known and appreciated due to its flexible and customized manufacturing capabilities. The widely studied RP techniques include stereolithography apparatus (SLA), selective laser sintering (SLS), three-dimensional printing (3DP), fused deposition modeling (FDM), 3D plotting, solid ground curing (SGC), multiphase jet solidification (MJS), laminated object manufacturing (LOM). Different techniques are associated with different materials and/or processing principles and thus are devoted to specific applications. RP technology has no longer been only for prototype building rather has been extended for real industrial manufacturing solutions. Today, the RP technology has contributed to almost all engineering areas that include mechanical, materials, industrial, aerospace, electrical and most recently biomedical engineering. This book aims to present the advanced development of RP technologies in various engineering areas as the solutions to the real world engineering problems.

How to reference

In order to correctly reference this scholarly work, feel free to copy and paste the following:

Takuma Nakano and Fumihito Arai (2011). Circulation Type Blood Vessel Simulator Made by Microfabrication, Advanced Applications of Rapid Prototyping Technology in Modern Engineering, Dr. M. Hoque (Ed.), ISBN: 978-953-307-698-0, InTech, Available from: http://www.intechopen.com/books/advanced-applications-of-rapid-prototyping-technology-in-modern-engineering/circulation-type-blood-vessel-simulator-made-by-microfabrication

INTECH
open science | open minds

InTech Europe
University Campus STeP Ri
Slavka Krautzeka 83/A
51000 Rijeka, Croatia
Phone: +385 (51) 770 447
Fax: +385 (51) 686 166
www.intechopen.com

InTech China
Unit 405, Office Block, Hotel Equatorial Shanghai
No.65, Yan An Road (West), Shanghai, 200040, China
中国上海市延安西路65号上海国际贵都大饭店办公楼405单元
Phone: +86-21-62489820
Fax: +86-21-62489821

© 2011 The Author(s). Licensee IntechOpen. This chapter is distributed under the terms of the Creative Commons Attribution-NonCommercial-ShareAlike-3.0 License, which permits use, distribution and reproduction for non-commercial purposes, provided the original is properly cited and derivative works building on this content are distributed under the same license.

IntechOpen

IntechOpen